The 28th Iranian Conference on Optics and Photonics (ICOP 2022), and the 14th Iranian Conference on Photonics Engineering and Technology (ICPET 2022). Shahid Chamran University of Ahvaz, Khuzestan, Iran, Feb. 1-3, 2022

لیزر دو ترازی از زاویه ای دیگر

بابک پروین

مراغه، دانشگاه مراغه، دانشکده علوم پایه، گروه فیزیک، صندوق پستی ۸۳۱۱۱-۵۵۱۸۱

چکیده- رفتار یک اتم دو ترازی به دام افتاده در یک کاوک اپتیکی تک مد در حالت پایا بررسی شده است. معادله اصلی توصیف کننده سامانه در پایه های اتم-کاواک از لحاظ عددی حل شده است. رفتارهای نیمه کلاسیکی و کوانتومی در سامانه اتم-کاواک بر اساس معادلات نوشته شده قابل استخراج می باشد. نتایج شبیه سازی های منتج شده از معادله اصلی، صحت این دو رفتار مجزا را تایید می کند.

کلید واژه–اتم دو ترازی، فوتون پاد خوشه ای، کاواک اپتیکی، لیزینگ، ماتریس چگالی.

A Two-Level Laser from Another Viewpoint

Babak Parvin

Physics Department, Faculty of Basic Sciences, University of Maragheh, P.O. Box 55181-83111

parvin@maragheh.ac.ir

Abstract- The behavior of a two-level atom trapped in a single-mode optical cavity is examined in the steady state. The describing master equation of the system is numerically solved in the atom-cavity basis. The semiclassical and quantum treatments in the atom-cavity system can be derived based on the written equations. The outcomes of the simulations resulting from the master equation confirm the accuracy of these two separate behaviors.

Keywords: density matrix, lasing, optical cavity, photon antibunching, two-level atom.

1. Introduction

In completing the topics given in [1], another method in solving the master equation is mentioned here. In the previous work [1] to solve the describing master equation of the atom-cavity system, a combination of the continued fractions and quantum optics toolbox methods was used, but here to solve the same equation, the method of solving equations in the atom-cavity basis has been utilized. Due to the lack of space, not all content can be illustrated here and [1] can be referred for a more complete detail.

2. Model

A two-level atom enclosed in a single-mode optical cavity. The 1-2 atomic transition is incoherently pumped at the rate of Γ'. The atom-cavity coupling constant is g and the 1-2 atomic transition frequency is at the resonance with the cavity one. The spontaneous emission coefficient from level 2 to 1 is equal to γ and the cavity decay rate is κ. The master equation of the atom-cavity system is:

$$\begin{aligned}\dot{\rho} &= \left[g\left(a\hat{A}_{21} - a^{\dagger}\hat{A}_{12} \right), \rho \right] \\ &+ \frac{\Gamma'}{2}\left(2\hat{A}_{21}\rho\hat{A}_{12} - \hat{A}_{11}\rho - \rho\hat{A}_{11} \right) \\ &+ \frac{\gamma}{2}\left(2\hat{A}_{12}\rho\hat{A}_{21} - \hat{A}_{22}\rho - \rho\hat{A}_{22} \right) \\ &+ \frac{\kappa}{2}\left(2a\rho a^{\dagger} - a^{\dagger}a\rho - \rho a^{\dagger}a \right),\end{aligned} \tag{1}$$

by using the master equation, the temporal evolution of the underneath quantities can be written as:

$$\dot{A}_{11} = -g\left\langle \hat{A}_{12}a^{\dagger} \right\rangle - g\left\langle \hat{A}_{21}a \right\rangle - \Gamma' A_{11} + \gamma A_{22}, \tag{2}$$

$$\dot{A}_{12} = g\left\langle \hat{A}_{11}a \right\rangle - g\left\langle \hat{A}_{22}a \right\rangle - 0.5\left(\Gamma' + \gamma \right) A_{12}, \tag{3}$$

$$\dot{A}_{22} = g\left\langle \hat{A}_{21}a \right\rangle + g\left\langle \hat{A}_{12}a^{\dagger} \right\rangle + \Gamma' A_{11} - \gamma A_{22}, \tag{4}$$

$$\dot{\alpha} = -gA_{12} - 0.5\kappa\alpha, \tag{5}$$

in the semiclassical approximation in which the correlations of the atom and cavity can be ignored, the above equations take this form:

$$\dot{A}_{11} = -gA_{12}\alpha^{*} - gA_{21}\alpha - \Gamma' A_{11} + \gamma A_{22}, \tag{6}$$

$$\dot{A}_{12} = gA_{11}\alpha - gA_{22}\alpha - 0.5\left(\Gamma' + \gamma \right) A_{12}, \tag{7}$$

$$\dot{A}_{22} = gA_{21}\alpha + gA_{12}\alpha^{*} + \Gamma' A_{11} - \gamma A_{22}, \tag{8}$$

$$\dot{\alpha} = -gA_{12} - 0.5\kappa\alpha, \tag{9}$$

by replacing $A_{21} = A_{12}$ and $\alpha^{*} = \alpha$ in the above equations, we will have:

$$\dot{A}_{11} = -2gA_{12}\alpha - \Gamma' A_{11} + \gamma A_{22}, \tag{10}$$

$$\dot{A}_{12} = gA_{11}\alpha - gA_{22}\alpha - 0.5\left(\Gamma' + \gamma \right) A_{12}, \tag{11}$$

$$\dot{A}_{22} = 2gA_{12}\alpha + \Gamma' A_{11} - \gamma A_{22}, \tag{12}$$

$$\dot{\alpha} = -gA_{12} - 0.5\kappa\alpha, \tag{13}$$

by eliminating the first level population, we have:

$$\dot{A}_{12} = g\alpha - 2gA_{22}\alpha - 0.5\left(\Gamma' + \gamma \right) A_{12}, \tag{14}$$

$$\dot{A}_{22} = 2gA_{12}\alpha + \Gamma' - \left(\Gamma' + \gamma \right) A_{22}, \tag{15}$$

$$\dot{\alpha} = -gA_{12} - 0.5\kappa\alpha, \tag{16}$$

after solving the above equations in the steady state, we arrive at $m = 0$ or:

$$m = -0.5p^{2} + \left(0.5N_{A}^{-1} - 1 \right) p - 0.5\left(N_{A}^{-1} + 1 \right), \tag{17}$$

in the above relations, these parameters $N_{A} = \kappa\gamma / \left(4g^{2} \right)$, $N_{\gamma} = \gamma^{2} / \left(4g^{2} \right)$, $p = \Gamma' / \gamma$, $m = n / N_{\gamma}$ and $n = \left| \alpha \right|^{2}$ are applied. The numerical value of $N_{A} = 0.05$ is applied in all diagrams in the subsequent sections.

3. Atom-Cavity Basis

To compare the semiclassical pattern with a completely quantum model, we examine the behaviour of the system at an arbitrary pumping $p = 1.5p_{1}$, where p_{1} is the smaller root of Eq. (17) which reveals the laser threshold. In the atom-cavity basis, the temporal evolution of the different elements of the density matrix are obtained from:

$$\begin{aligned}\dot{\rho}_{n,1;n,1} &= -g\sqrt{n}\rho_{n-1,2;n,1} - g\sqrt{n}\rho_{n,1;n-1,2} \\ &- \left(\Gamma' + \kappa n \right) \rho_{n,1;n,1} + \gamma\rho_{n,2;n,2} \\ &+ \kappa\left(n+1 \right) \rho_{n+1,1;n+1,1},\end{aligned} \tag{18}$$

$$\dot{\rho}_{n-1,2;n,1} = g\sqrt{n}\rho_{n,1;n,1} - g\sqrt{n}\rho_{n-1,2;n-1,2} -0.5\left(\Gamma' + \gamma + \kappa(2n-1)\right)\rho_{n-1,2;n,1} +\kappa\sqrt{n(n+1)}\rho_{n,2;n+1,1}, \tag{19}$$

$$\dot{\rho}_{n,2;n,2} = g\sqrt{n+1}\rho_{n+1,1;n,2} + g\sqrt{n+1}\rho_{n,2;n+1,1} +\Gamma'\rho_{n,1;n,1} - (\gamma + \kappa n)\rho_{n,2;n,2} +\kappa(n+1)\rho_{n+1,2;n+1,2}, \tag{20}$$

which form a closed and infinite set of equations. To solve these equations in the steady state, by truncating these equations in an arbitrary n such as N, those can be brought into $Ax = b$ and finally one can obtain the unknown matrix x. When the answer of x is acceptable that its values do not change for $N-1$ and $N+1$. By specifying the matrix x, the following physical quantities can be obtained:

$$A_{22} = \left\langle \hat{A}_{22} \right\rangle, \tag{21}$$

$$m = \left\langle a^{\dagger} a \right\rangle / N_{\gamma}, \tag{22}$$

$$g^{(2)}(0) = \left\langle a^{\dagger^2} a^2 \right\rangle / \left\langle a^{\dagger} a \right\rangle^2, \tag{23}$$

which indicates the second level population, scaled photon number and second-order coherence function at zero-time delay, respectively. In Fig. 1, the scaled photon number curves are plotted in two separate intervals. The depicted results show that for large N_{γ}'s the semiclassical behaviours prevail in the system and with decreasing N_{γ}, the deviation from the semiclassical case increases and the quantum processes are expected to appear in the system.

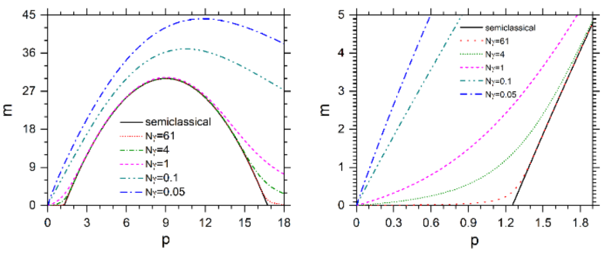

Fig. 1: The curves of m for different N_{γ}'s along with the semiclassical case in terms of p at two various intervals

In Fig. 2, the second-order coherence function is used to determine the behaviour of the emitted light. For the largest N_{γ}, at below threshold, the radiated light is thermal and becomes coherent at above threshold and gets thermal again as the pump increases further. As N_{γ} decreases the light becomes bunched. For the lowest N_{γ} and in the weak driving limit, the light denotes the antibunching characteristic. Therefore, the results of this section display that for large enough N_{γ}'s, the behaviours of the semiclassical laser emerge in the system and for small enough N_{γ}'s and in the weak driving limit, the antibunched light is emitted which is a quantum light. The drawn outcomes in Figs. 1 and 2 are in complete agreement with those of [1].

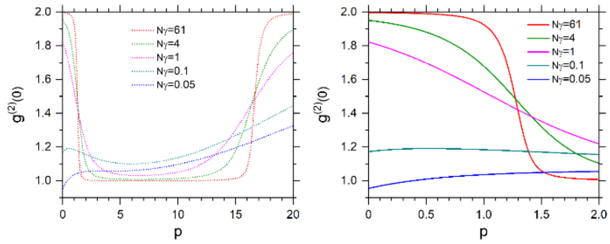

Fig. 2: The graphs of $g^{(2)}(0)$ for several N_{γ}'s versus p in two different domains

4. Photon Antibunching

Here we want to see that what quantum effects appear in the system for small N_{γ}'s. In the weak driving limit $\Gamma' \ll \gamma$ which is equivalent to $p \ll 1$, Eqs. (18) to (20) can be expanded to the second order of Γ'. Using these equations, one can say that $\rho_{n,1;n,1}$ and $\rho_{n-1,2;n,1}$ are of the order of n with respect to Γ' and $\rho_{n,2;n,2}$ is of the order of $n+1$. By opening the given equations to the leading order:

$$\dot{\rho}_{0,1;0,1} = -\Gamma'\rho_{0,1;0,1} + \gamma\rho_{0,2;0,2} + \kappa\rho_{1,1;1,1}, \tag{24}$$

$$\dot{\rho}_{1,1;1,1} = -g\rho_{0,2;1,1} - g\rho_{1,1;0,2} - \kappa\rho_{1,1;1,1}, \tag{25}$$

$$\dot{\rho}_{2,1;2,1} = -g\sqrt{2}\rho_{1,2;2,1} - g\sqrt{2}\rho_{2,1;1,2} - 2\kappa\rho_{2,1;2,1}, \tag{26}$$

$$\dot{\rho}_{0,2;1,1} = g\rho_{1,1;1,1} - g\rho_{0,2;0,2} - 0.5(\gamma + \kappa)\rho_{0,2;1,1}, \tag{27}$$

$$\dot{\rho}_{1,2;2,1} = g\sqrt{2}\rho_{2,1;2,1} - g\sqrt{2}\rho_{1,2;1,2} \\ -0.5(\gamma+3\kappa)\rho_{1,2;2,1}, \tag{28}$$

$$\dot{\rho}_{0,2;0,2} = g\rho_{1,1;0,2} + g\rho_{0,2;1,1} + \Gamma'\rho_{0,1;0,1} - \gamma\rho_{0,2;0,2}, \tag{29}$$

$$\dot{\rho}_{1,2;1,2} = g\sqrt{2}\rho_{2,1;1,2} + g\sqrt{2}\rho_{1,2;2,1} + \Gamma'\rho_{1,1;1,1} \\ -(\gamma+\kappa)\rho_{1,2;1,2}, \tag{30}$$

which from a closed set of equations. In the weak driving limit, the population of the first level to the first order of Γ' can be written as:

$$\rho_{0,1;0,1} + \rho_{1,1;1,1} = 1, \tag{31}$$

by solving these equations in the steady state:

$$\rho_{0,1;0,1} = \frac{(\gamma+\kappa)(1+N_A)}{(\gamma+\kappa)(1+N_A)+\Gamma'}, \tag{32}$$

$$\rho_{1,1;1,1} = \frac{\Gamma'}{(\gamma+\kappa)(1+N_A)}\rho_{0,1;0,1}, \tag{33}$$

$$\rho_{0,2;0,2} = \left(1+\frac{\kappa}{4g^2}(\gamma+\kappa)\right)\rho_{1,1;1,1}, \tag{34}$$

$$\rho_{2,1;2,1} = \frac{\Gamma'}{(\gamma+3\kappa)\left(1+\frac{\kappa}{4g^2}(\gamma+\kappa)\right)}\rho_{1,1;1,1}, \tag{35}$$

now the second level population, second-order coherence function to the leading order are derived from:

$$A_{22} \simeq \frac{(N_\gamma + N_\gamma N_A + N_A^2)p}{N_\gamma + N_\gamma N_A + N_A + N_A^2 + N_\gamma p}, \tag{36}$$

$$g^{(2)} \simeq \frac{2N_\gamma(N_\gamma p + N_\gamma + N_A + N_A N_\gamma + N_A^2)}{N_\gamma^2 + N_A N_\gamma^2 + 4N_\gamma N_A^2 + 3N_A N_\gamma + 3N_A^3}, \tag{37}$$

which relation (37) is equal to that one written in [1]. Now the above functions can be plotted under these conditions $N_A \ll 1$ and $N_\gamma \ll N_A^2$, although to apply these conditions the two variables Taylor expansion method can be used similar to that of used in [1], but here this method is not applied since the mentioned approximations show their effects directly on the drawn curves. In Fig. 3(a), the curves of $g^{(2)}(0)$ are depicted for different N_γ's against p. The dashed curves are plotted according to Eq. (23) and the solid lines are drawn based on Eq. (37). With the decline of N_γ, the obtained results become closer and closer to those of the simulations and stronger antibunching phenomenon occurs.

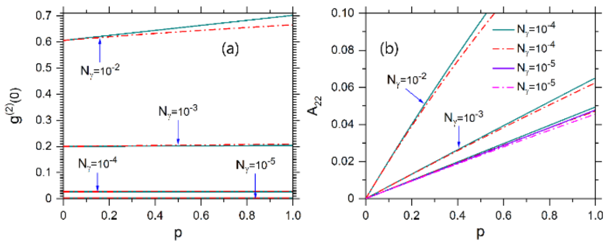

Fig. 3: (a) The emergence of photon antibunching effects, (b) The population of the second atomic level in two distinct cases for small N_γ's in terms of p

In Fig. 3(b), the A_{22} curves are drawn for some N_γ's versus p. The solid lines are plotted according to Eq. (36) and the dashed diagrams are depicted based on Eq. (21). By reducing N_γ, the achieved results become close to the simulation ones and this indicating that the applied approximations in this section are acceptable.

5. Conclusions

In this work, the different behaviours of the two-level atom enclosed in the single-mode optical cavity are theoretically examined. The master equation describing the atom-cavity system is solved numerically in the density matrix basis. The results show that for large N_γ's, the system unravels the behaviour of the semiclassical laser, and for small N_γ's and in the weak driving limit, the photon antibunching quantum feature appears in the system. The brought results appropriately verify the obtained findings in [1] which applied other approaches to solve the master equation.

References

[1] B. Parvin, "Lasing and nonlasing regimes in a two-level laser," Eur. Phys. J. Plus, Vol. 136, pp. 728 (1-13), 2021 and references therein.